Shiraz E-Med J. 2023 September; 24(9):e136960. https://doi.org/10.5812/semj-136960.

Published online 2023 October 8. **Research Article**

Effect of Platelet-rich Plasma Combined with Marburg Bone Bank-prepared Bone Graft in Rabbit Bone Defect Model

Dina Saginova [1], Elyarbek Tashmetov [2,*], Berik Tuleubaev [2], Yevgeniy Kamyshanskiy [3] and Sherzad Davanov [4]

[1]The Center for Applied Scientific Research, National Scientific Center of Traumatology and Orthopaedics Named After Academician N.D.Batpenov, Nur-Sultan, Kazakhstan
[2]Department of Surgical Diseases, Karaganda Medical University, Karaganda, Kazakhstan
[3]Pathology Unit of the University Clinic, Karaganda Medical University, Karaganda, Kazakhstan
[4]Department of Ambulance, Anesthesiology and Resuscitation, Karaganda Medical University, Karaganda, Kazakhstan

[*]*Corresponding author*: Department of Surgical Diseases, Karaganda Medical University, Karaganda, Kazakhstan. Email: tashmetov.e@gmail.com

Received 2023 April 19; **Revised** 2023 September 02; **Accepted** 2023 September 10.

Abstract

Background: An effective technique for inducing bone formation without using an autograft has yet to be established. Platelet-rich plasma (PRP), which can be obtained easily from whole blood, contains substantial growth factors (GFs) that can facilitate bone regeneration and growth.
Objectives: This study aimed to evaluate the effect of PRP combined with a Marburg bone bank-prepared bone graft in a rabbit bone defect model.
Methods: This study utilized 32 rabbits (n = 16 in each group). Bone defects were intentionally made in the femur, and the bone allograft used was the human femoral head prepared according to the Marburg bone bank. Rabbits were divided into Marburg bone graft (MBG) and MBG+PRP groups. Histopathological and histomorphometric analyses were conducted 14 and 30 days post-surgery.
Results: A greater new bone formation was detected in both groups on the 14th and 30th days (P = 0.001). Furthermore, more pronounced angiogenesis was found in the MBG+PRP group than in the MBG group (P = 0.001).
Conclusions: The MBG-PRP complex significantly enhanced bone tissue repair in bone defects. The inclusion of PRP was found to promote angiogenesis and stimulate the formation of new bone tissue, further supporting the beneficial effects of this combination in the healing process.

Keywords: Bone Graft, Bone Defect, Platelet-rich Plasma, Marburg Bone Bank System

1. Background

Bone defects commonly manifest as a result of bone resection, metabolic pathologies, traumatic events, and neoplasms. Annually, these osseous deficiencies necessitate more than one million reconstructive surgical interventions (1, 2). The main principle of treating defects of any etiology is filling with bone fillers. Autologous bone for filling is the "gold standard" (3, 4). First, the autologous bone does not cause any immunological reactions. Second, it has simultaneously both osteoinductive and osteoconductive properties; the former is represented by bone cells and growth factors. The limited availability of acquired autologous bone and the accompanying trauma induced by the harvesting procedure restricts its utilization in clinical practice (4, 5). A viable alternative involves the employment of bone allografts, which maintain the autograft's intrinsic osteoconductive characteristics while reducing the transmission of donor-host disease (6, 7).

The Marburg bone bank prepared bone graft is a bone allograft widely used in orthopedic surgery. These grafts are extensively processed to remove cellular material, leaving only the mineralized bone matrix behind. The processed bone matrix provides a scaffold for new bone growth, which can lead to faster and more complete healing (8-10). Nevertheless, the osteoinductive capability of processed (chemically or physically) allogeneic bone is not clearly established, given that osteogenic cells are eradicated during the tissue manipulation process. This leads to the partial retention of osteoinductive substances, which may contribute to suboptimal clinical effects.

Currently, there has been a surge in interest regarding the utilization of growth factors and morphogens as potential agents for conferring osteoinductivity to bone substitutes (11-14).

Platelet-rich plasma (PRP) obtained from autologous blood represents a significant resource for delivering high levels of growth factors, including platelet-derived growth factor (PDGF), transforming growth factor beta (TGF-b), epidermal growth factor (EGF), vascular endothelial growth factor (VEGF), and insulin-like growth factor I (IGF-I). These factors are vital in tissue growth and progression, and their introduction to the site of bone defects is crucial (15, 16). As known, PRP has the potential for use with bone grafts, as in vitro studies have demonstrated a notable increase in osteoblast proliferation upon the addition of PRP (15). Furthermore, incorporating PRP with graft materials can reduce the duration required for graft consolidation, maturation, and improvement of trabecular bone density (17-19). These findings suggest that PRP may compensate for the limited osteogenic potential of thermally disinfected bone grafts to promote osteogenesis in bone defects. However, there is limited information regarding the synergistic effects of PRP and Marburg-prepared bone grafts on bone healing.

2. Objectives

This study aimed to evaluate the effect of PRP in combination with a Marburg bone bank-prepared bone graft in the rabbit bone defect model.

3. Methods

The experimental study was undertaken at the Department of Surgical Diseases of Karaganda Medical University, while the histological and histopathological examinations were conducted at the Department of Pathology of the University Clinic of Karaganda Medical University. The study spanned from September 2021 to September 2022.

3.1. Preparation of Marburg Bone Grafts

In the present study, femoral heads prepared by the Marburg bank were employed as bone grafts (Figure 1). These femoral heads were obtained from a living donor who had undergone hip joint arthroplasty surgery in compliance with national regulations (20, 21). During hip joint endoprosthesis, the head of the femur was removed from the operating room and subjected to a series of mechanical cleaning procedures in sterile conditions to eliminate any soft tissue, cartilage, and ligaments. The cleaned femoral bone allografts were then perforated using a specially designed device at equal intervals (22). The femoral heads were placed in a disposable sterile container and filled with 0.9% NaCl solution in a volume of 300 mL, after which they were sealed and subjected to a heat treatment process in a Lobator SD-2 (Telos Company, Germany) device for a total of 94 minutes, maintaining a temperature of 82.5°C in the femoral head for at least 15 minutes, according to the established protocol. The sterility of the container was verified at the end of the cycle through a specific opening, after which the liquid was completely drained. The bone allografts were then stored in a freezer at -80°C per the recommended protocol (9). Two hours before the experiment, the femoral head was unfrozen at room temperature and cut into chips. To ensure a consistent ratio of ingredients, a specific weight was used to standardize the mixture of bone graft with PRP at 0.5 g bone allograft/0.5 mL PRP.

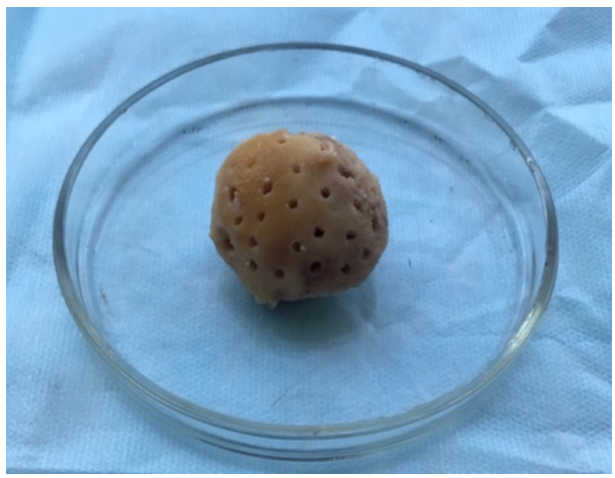

Figure 1. Heat-treated femoral head

3.2. Preparation of Platelet-rich Plasma

Approximately 30 minutes before each surgical intervention, 5 mL of blood was drawn from the hearts of rabbits in the PRP group. The blood was collected into siliconized tubes containing 3.8% sodium citrate at a blood-to-citrate ratio of 9:1 (23). The blood sampling procedure was performed under general anesthesia, which was induced by administering an intramuscular Zoletil injection at 0.1 mg/kg and Rometar at a dose of 5 mg/kg. Platelet-rich plasma was procured via two-step

centrifugation (24). Initial centrifugation involved the separation of blood cell elements using a laboratory centrifuge, with tubes centrifuged at 900 G for 5 minutes at ambient temperature, yielding two primary components: The blood cell component (BCC) in the lower fraction and the serum component (SC) in the upper fraction. Subsequent centrifugation entailed marking a point 6 mm beneath the line, demarcating the BCC and SC. All contents above the mark were transferred to another 5 mL vacuum tube devoid of anticoagulant to augment the total platelet count for the second centrifugation. The sample was then centrifuged once more at 1,500 G for 10 minutes to obtain SC and PRP components. Approximately 0.5 mL of PRP was separated from the SC. The PRP (0.5 mL) was combined with 0.5 g of bone graft and utilized to fill the created defect.

3.3. Animals and Surgical Procedures

In the present investigation, 32 outbred rabbits were acquired, comprising adult males (6 - 7 months old) with an average weight of 3,065 ± 63 g. The animals were housed in cages and allowed to acclimate for 2 weeks. All procedures involving the animals adhered to the Guide for the Care and Use of Laboratory Animals (25) and were sanctioned by the University Animal Care Committee (UACC) under protocol No. 27 dated 27.09.2020. Throughout the study, the rabbits were maintained at room temperature (22 ± 2°C), 40 - 50% humidity, and subjected to a 12-hour light-dark cycle. The animals were provided with standard rabbit pellets and tap water for sustenance.

Following Russell and Burch's bioethical principles of replacement, reduction, and refinement (1959) (26), the sample size for animal experimentation in this study was established as the minimum number of animals necessary to yield statistically significant outcomes (26).

The rabbits were randomly assigned to two groups (n = 16 per group) using a random number generator, and all underwent the same surgical procedure. Three hours before, the rabbits received an intramuscular (i.m.) injection of gentamycin 0.1 mL/kg (MAPICHEM, Switzerland). They were anesthetized with an intramuscular injection of Zoletil 0.1 mg/kg (Virbac, USA) and Rometar 5 mg/kg (Bioveta, Czech Republic). Following hip skin disinfection, an incision was made in the distal femur. The periosteum was then lifted, and a 5-mm-diameter bone defect was created in the distal femoral metaphysis using a drill (Figure 2) (27). Afterward, based on the experimental group assignment, the bone defects in group 1 were treated with a Marburg bone graft (MBG), whereas in group 2, the defects were treated with the Marburg bone graft and autologous PRP (MBG+PRP). The surgical wound was sutured with absorbable sutures (5-0 Vicryl, Ethicon, Johnson & Johnson, USA). After surgery, each animal received i.m. injections of gentamycin 0.1 mL/kg (MAPICHEM, Switzerland) and ketonal 0.04 mL/kg (Sandoz, Slovenia) for 3 days. Daily postoperative observations were conducted to monitor the healing progress on a predetermined schedule for consecutive days. There were no complications or deaths in the postoperative period. On 14 and 30 days, the animals were sacrificed according to ethical standards by intravenously administrating lethal doses of Zoletil 50 mg/mL, and the distal femur was harvested.

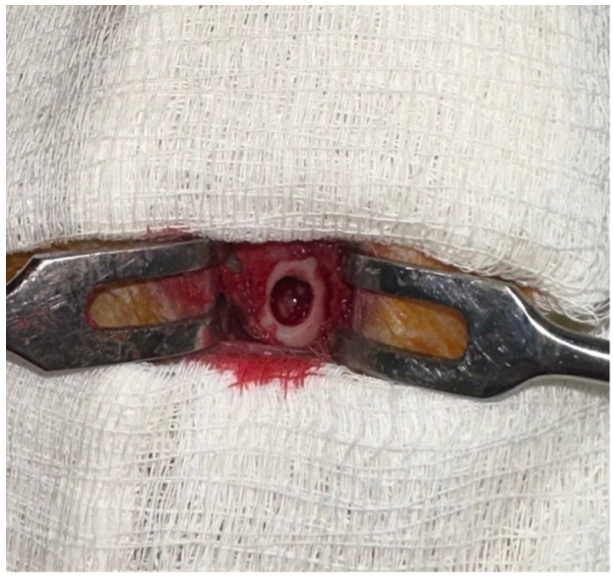

Figure 2. Bone defect in rabbit femur

3.4. Histopathological Examination

The object for histopathological examination was a bone fragment with a formed defect. Before histological analysis, the specimens were fixed in 10% neutral buffered formalin for 24 hours, followed by decalcification in Biodec R solution (Bio-Optica Milano SPA) for an additional 24 hours. Subsequently, the samples were rinsed in phosphate buffer (pH = 7.4). A bone incision was executed upon achieving optimal bone tissue softening (decalcification). The tissue was then fixed in 10% formalin at 4°C for 24 hours, washed with tap water, and dehydrated using a series of ascending alcohol concentrations (70%,

90%, 95%, and 100%). The samples were then immersed in xylene and embedded in paraffin blocks. Tissue sections with a thickness of 5 μm were prepared using a Leica SM 2000R sliding microtome. After preparation, the tissue sections were stained using hematoxylin and eosin staining to determine the general tissue morphology and the cellular composition of the bone defect and Masson's trichrome staining to determine the percentage of fibrous tissue, cartilage tissue, and bone tissue (28). Microscopic examination of the preparations was conducted on a Zeiss AxioLab 4.0 microscope with a magnification of x400. AxioVision 7.2 software for Windows was used to analyze and photograph the images. Calculation of the cellular composition of the bone plate defect (osteoclasts, osteoblasts, and osteocytes) was carried out in sections stained with hematoxylin and eosin: osteoclasts, osteoblasts, and osteocytes were counted per 1000 cells on the defect zone area, and the obtained mean values were expressed with an accuracy of 2 decimal places for each group. Morphometric assessment of fibrous, cartilaginous, and osseous tissue was conducted within the area delineated radially by the defect endpoints and laterally by the native femur and the external boundary of the bone graft and/or newly formed bone tissue. This evaluation was expressed as a percentage of the overall area of the defect zone. Three slices were evaluated for each bone defect, and the mean value was calculated. To determine the proportion of the defect area closure with bone and cartilage tissue, a horizontal line was plotted across the outer portion of the inner and outer cortical bone layer at the defect's edges. The presence of erythrocytes in the lumen and endothelial cell lining characterized blood vessels, and the number of vessels per defect area was estimated based on 10 fields of view at $\times$200 magnification. Two certified histologists blinded to the group allocation conducted histological analysis using a histological bone defect healing score (Table 1).

Table 1. Histopathological Parameters of Bone Defect Healing Score

	Histological Score
Inflammation	Polymorphonuclear leukocytes [a]
	Lymphocytes [a]
	Macrophages/Histiocytes [a]
Cellular composition	Osteoblasts [b]
	Osteocytes [b]
	Osteoclasts [b]
Tissue composition	Fibrous tissue (%)
	Cartilage (%)
	Bone (%)
Vessels	Neovascularization [c]

[a] Cellular infiltration was evaluated on 100 cells by summing the mean values of various cell types in the defect zone area.
[b] Assessment of the cellular composition was conducted for 1,000 cells by summing the average values of different cell types around the defect zone.
[c] Examination of the number of newly formed vessels was carried out on the area of the created defect, calculated for 10 fields of view.

3.5. Statistical Analysis

Descriptive statistics for each group were presented using the mean, frequency, standard error of the mean (SE), or percentage of the respective parameter. To assess differences between groups, we employed the Student's *t*-test and the Mann-Whitney test, taking into account the validation of the usual assumptions for all parameters. The research results were analyzed using IBM SPSS Statistics 20.0 and STATISTICA 10. A P-value of <0.05 was deemed to indicate statistical significance.

4. Results

Histological characteristics of the cellular composition of the bone plate defect after 14 days showed that the average number of osteoblasts in the MBG group was 298.5 ± 8.5 cells, the average number of osteoclasts was 10.0 ± 7.4 cells, and the average number of osteocytes was 213.8 ± 5.7 cells per 1000 cells in the defect zone (Figure 3). In the MBG+PRP group, the mean number of osteoblasts and osteocytes was significantly greater than that in the MBG group (P = 0.001), while no difference was found in the number of osteoclasts (P = 0.189). In contrast, on the 30th day, the number of osteoclasts was significantly higher in the MBG group than in the MBG+PRP group (P = 0.011). There was a significant difference between the MBG and MBG+PRP groups in terms of the number of osteoblasts and osteocytes ($P < 0.001$) (Figure 3).

Histological and morphometric characteristics of the tissue composition of the bone plate defect (staining with Masson's trichrome)

In the MBG group, after 14 days, animals were characterized by forming a new bone in the place of the formed defect (Figure 4A). The new osseous tissue was viable, comprising lacunae replete with osteocytes and a profusion of vascular channels. Histologically, the newly formed bone's trabecular matrix was interconnected with the graft's bone. Bone tracts of newly formed bone tissue are heterogeneous and predominantly thin, with focal bridge-like areas and single contacts, mainly at the poles of the bone tracts.

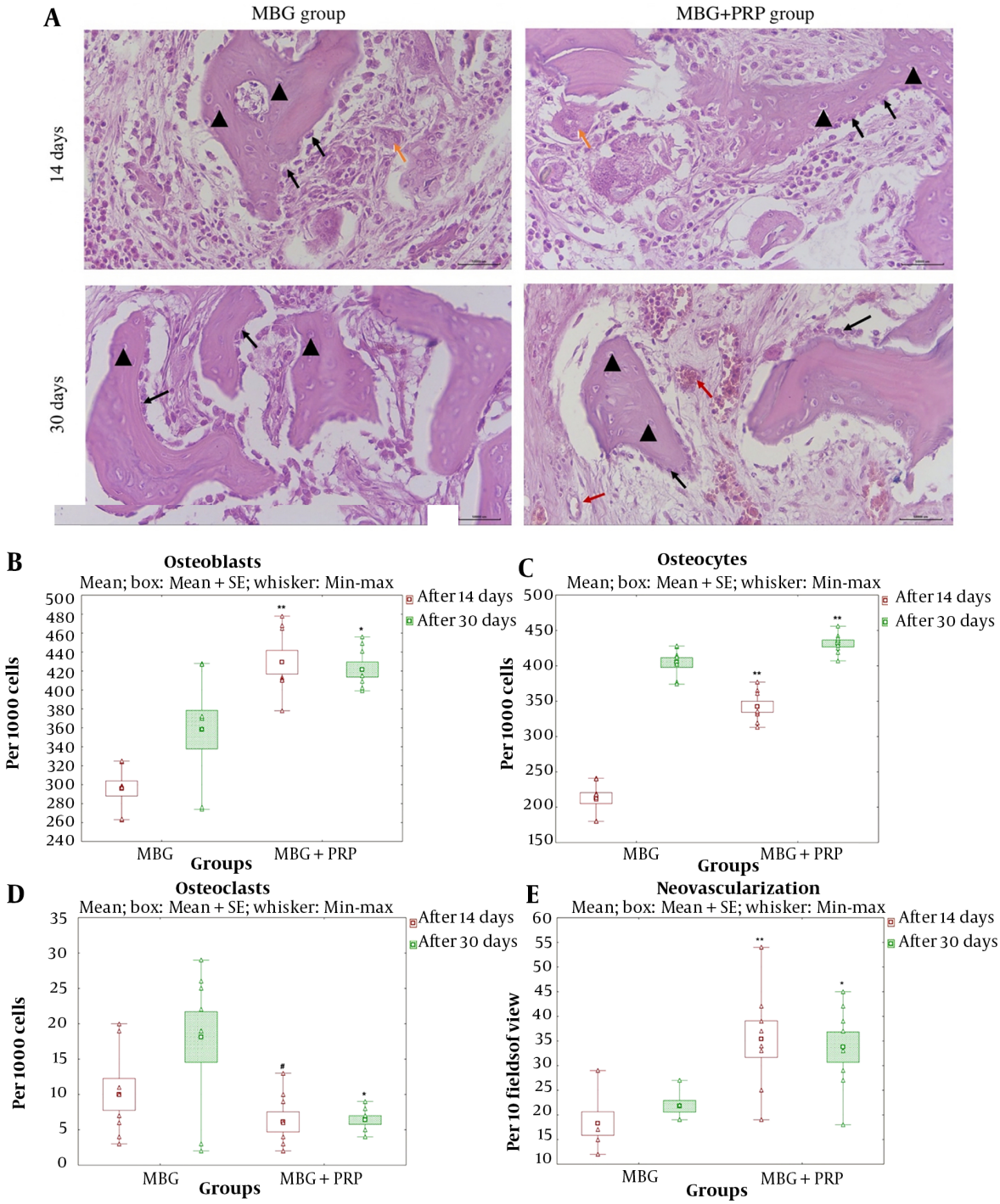

Figure 3. Characteristics of cellular composition after 14 and 30 days: (A) osteoblasts (black arrow) and giant multinucleated cells (orange arrow) are observed on the bone surface, along with osteocytes (black arrowhead) and newly formed vessels in connective tissue (red arrow) (HE × 400); (B) comparison of the number of osteoblasts between groups; (C) comparison of the number of osteocytes between groups; (D) comparison of the number of osteoclasts between groups; (E) comparison of neovascularization between groups. (*P < 0.01; **P < 0.001; #P > 0.05)

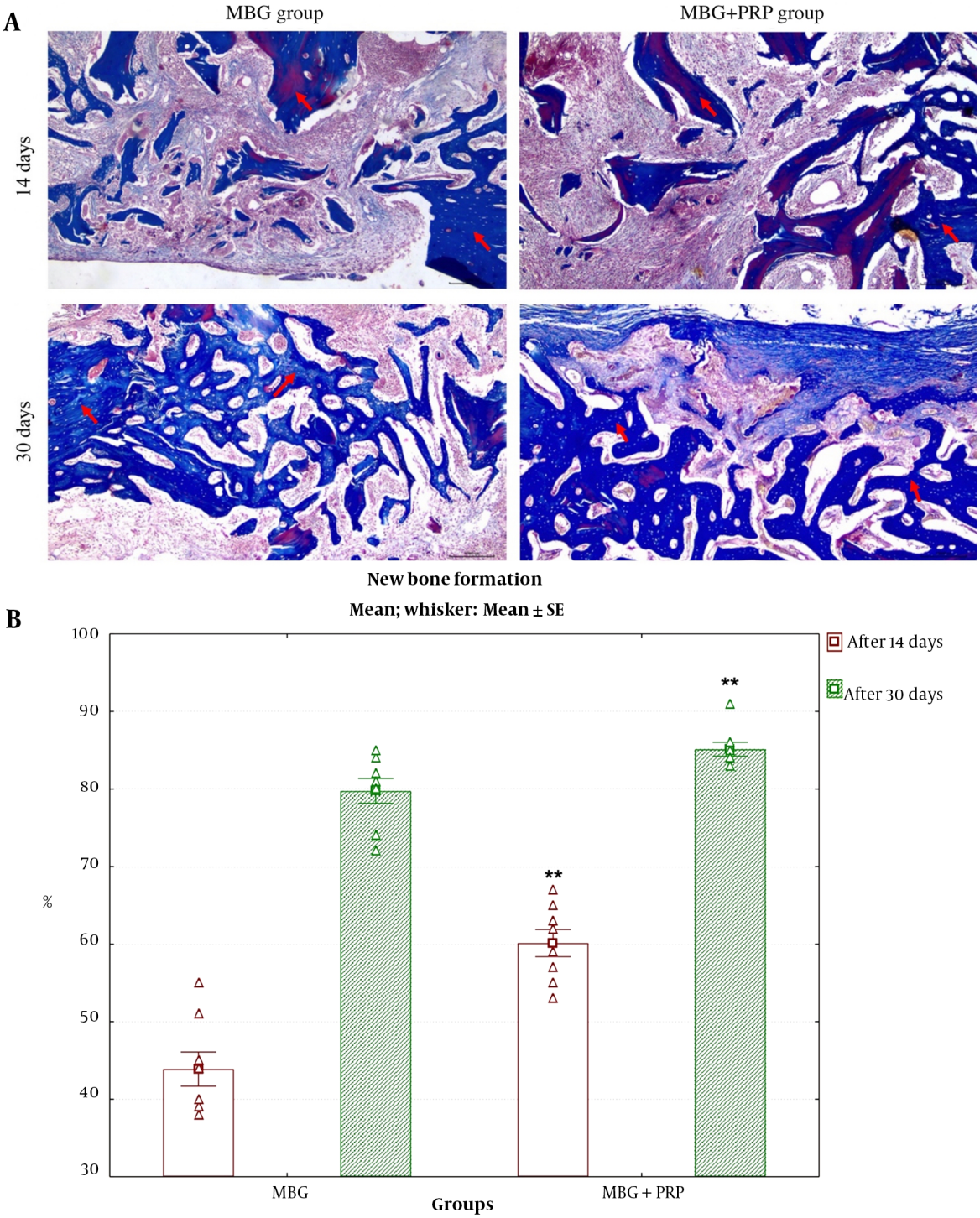

Figure 4. Histological pattern of newly formed bone tissue in the defect area after 14 and 30 days: (A) the defect zone is closed with fibrous tissue and newly formed bone trabeculae (red arrow) extending from the edge of the defect in the bone plate; (B) comparison of the amount of bone tissue between groups. (**P < 0.001)

The presence of fibrous tissue was characterized by the focal formation of coarse fibrous connective tissue fibers, predominantly at the periphery of the bone allograft, without spreading beyond the representative area of the bone defect (Figure 4A). In the MBG+PRP group, the bone defect healing rate was significantly higher than in the MBG group (Figure 4B) (Appendix 1 in the Supplementary File). The morphological features indicating the reparative process in the cortical layer of the bone were defined by a gradual augmentation of fully developed osseous tissue, along with randomly situated Haversian canals and horizontally spanning bone trabeculae. The bone trabeculae of the newly formed bone tissue are wide, with multiple wide bridge-like contacts between the newly formed bone trabeculae. Multiple vascular bundles were observed in the area of bone defect in both groups. However, the neovascularization rate was higher in the MBG group.

On day 30, the MBG group demonstrated bone tissue identification via a condensed basophilic line and detection of osteocytes in the lacunae of the recently generated bone. Bone tissue was exhibited in the configuration of arbitrarily located bone trabeculae and strands that congregate to form lamellar structures. The bone tracts displayed a notable level of mineralization and vigorous longitudinal growth. In the MBG+PRP group, on day 30, the new bone formation was greater than in the MBG group, and the defect zone was represented by compact mineralized bone tissue with Haversian canals of various sizes and neovascularization (Figure 4).

The MBG group exhibited a focal and disordered pattern of neovascularization, whereas the MBG+PRP group demonstrated a consistent and uniform distribution.

Neither the MBG nor the MBG+PRP group exhibited any indications of chondroid or bone callus hyperplasia on the histological sections. Instead, thin layers of fibrous tissue and blood vessels, as well as varying degrees of resorption of the bone graft, were observed, along with osteoclasts and fibrovascular structures. These observations were comparable in both groups, and using PRP caused no supplementary histological alterations.

5. Discussion

This study analyzes the cellular and tissue composition and the reparative pattern of the newly formed bone after using a Marburg bone bank-prepared bone graft with and without PRP in an animal experiment. The analysis involved histopathological and histomorphometric examinations.

First, we showed that using PRP with thermally disinfected bone graft improves and enhances osteogenesis compared with the group of bone grafts without additional biocomponents. Thus, there was a relatively larger number of osteoblasts in the group with PRP on the 14th and 30th days, in contrast to those without PRP ($P < 0.001$). Osteoblasts circularly lined the bone fragments of the bone graft with newly formed bone tissue and the formation of multiple bundles of accumulation of osteoblastic cells with multidirectional growth of bone tissue with a more pronounced phenomenon of "bridging" of bone fragments. Also, in the group with PRP on day 30 (Figure 4), the relative number of maturing and mature bone tissue cells was statistically significantly higher than in the group with only bone graft.

Previously, it was shown that PRP improves the regenerative properties of connective and epithelial tissue by increasing the activity of fibroblast-like cells and stimulating cell proliferation (29-33). We believe that bone graft, in combination with PRP, improves osteoconductive potential and induces an osteoinductive effect, which is reflected in the enhancement and acceleration of growth and maturation of bone tissue in the defect area.

Previously, it was discovered that, in addition to osteoblasts and osteoclasts, which have traditionally been considered the main contributors to bone remodeling processes, osteocytes also play a significant role in regulating and controlling these processes (34-36). The action of osteocytes forms a "controlled bone strategy" aimed at bone repair and remodeling (37, 38). Osteocytes generate signals that modulate the functioning of osteoblast cells, which in turn regulate bone modeling and promote the development of fresh bone tissue (39, 40). In vitro investigations have indicated that osteocytes function as a suppressor of osteoclast activity and could potentially play a crucial role in initiating localized bone restructuring (37, 41). A sufficient number of living osteocytes is an obligatory condition for the remodeling activity of bone tissue in the defect zone. The higher osteocyte count found in the present study in bone with PRP than in bone graft suggests that PRP improves bone repair and remodeling.

Second, we showed that PRP improves angiogenesis in the area of bone defects. When analyzing the reparative pattern, we found that the relative number of microvessels in the PRP group was statistically significantly higher (Figure 3E) ($P < 0.001$) than in the group without PRP.

In the PRP group, microvessels had a relatively uniform distribution over the entire defect zone for 14 days, while in the group without PRP, active angiogenesis was uneven and more densely observed in the peripheral zones of the defect. The process of angiogenesis is significant and necessary for tropism, growth, and maturation of bone tissue (42-44). It was previously reported that PRP use in soft tissue regeneration enhances angiogenesis, which is its main bioeffect (43). We found that in our groups, more dense zones of maturing and mature bone tissue were formed in zones with a relatively large number of microvessels. We believe that the PRP-induced effect of bone growth and maturation activity is more likely associated with a direct effect on angiogenesis and indirectly on an osteoinductive effect.

Further, we showed that in the PRP group, there were no abnormalities in bone repair associated with insufficient or excessive bone formation. Newly formed bone tissue in both groups was characterized by normal his pattern: (1) the bone plate did not extend beyond the thickness of the bone defect and did not pass to the bone plate outside the defect, (2) it had a laminar layered structure with a focal chaotic pattern in the area of predominantly Haversian canals, and (3) the relative amount of bone tissue and Haversian canals did not differ both between groups and from the structure of the bone outside the bone defect.

The strength of this study is the comparative characteristics of using thermally treated bone grafts with PRP, which made it possible to identify the positive aspects of PRP in bone regeneration. However, the direct effect of PRP on bone tissue remains debatable. Does it act directly on osteosynthesis and bone maturation or indirectly through forming a favorable macro-environment with a high angiogenesis index? The answers to these questions can be obtained in further research.

5.1. Conclusions

The PRP-thermally treated bone graft complex improves bone tissue repair in the zone of the induced defect in experimental rabbits. It was revealed that PRP enhances the process of angiogenesis and the formation of newly formed bone tissue. We believe that the main effect of improving the osteoconductive and osteoinductive potentials of the PRP graft is associated with the formation of a locoregional favorable microenvironment with an active perfusion and diffusion potential of the stromal framework, which contributes to more active growth and maturation of bone tissue.

Supplementary Material

Supplementary material(s) is available here [To read supplementary materials, please refer to the journal website and open PDF/HTML].

Footnotes

Authors' Contribution: S. D. supervised the study, designed the study, re-evaluated the experimental data, and revised the manuscript. E.T. conceived and designed the study and evaluation and drafted the manuscript. Ye. K. participated in designing the evaluation, performed parts of the statistical analysis, and helped draft the manuscript. B. T. collected the data, interpreted them, and revised the manuscript. Sh. D. performed the experiments and helped to draft the manuscript. All authors read and approved the final manuscript.

Conflict of Interests: The authors declare that there is no conflict of interest.

Data Reproducibility: The datasets generated and/or analyzed during the current study are available from the corresponding author upon reasonable request.

Ethical Approval: The animal study protocol was approved by the University Animal Care Committee (UACC) of Karaganda Medical University (protocol No. 27 27.09.2020).

Funding/Support: This research has been funded by the Science Committee of the Ministry of Education and Science of the Republic of Kazakhstan (Grant No. AP09260954).

References

1. Winkler T, Sass FA, Duda GN, Schmidt-Bleek K. A review of biomaterials in bone defect healing, remaining shortcomings and future opportunities for bone tissue engineering: The unsolved challenge. *Bone Joint Res*. 2018;**7**(3):232–43. [PubMed ID: 29922441]. [PubMed Central ID: PMC5987690]. https://doi.org/10.1302/2046-3758.73.BJR-2017-0270.R1.
2. Molina CS, Stinner DJ, Obremskey WT. Treatment of Traumatic Segmental Long-Bone Defects: A Critical Analysis Review. *JBJS Rev*. 2014;**2**(4). [PubMed ID: 27490871]. https://doi.org/10.2106/JBJS.RVW.M.00062.
3. Fillingham Y, Jacobs J. Bone grafts and their substitutes. *Bone Joint J*. 2016;**98-B**(1 Suppl A):6–9. [PubMed ID: 26733632]. https://doi.org/10.1302/0301-620X.98B.36350.
4. Chiarello E, Cadossi M, Tedesco G, Capra P, Calamelli C, Shehu A, et al. Autograft, allograft and bone substitutes in reconstructive orthopedic surgery. *Aging Clin Exp Res*. 2013;**25 Suppl 1**:S101–3. [PubMed ID: 24046051]. https://doi.org/10.1007/s40520-013-0088-8.

5. Lauthe O, Soubeyrand M, Babinet A, Dumaine V, Anract P, Biau DJ. The indications and donor-site morbidity of tibial cortical strut autografts in the management of defects in long bones. *Bone Joint J*. 2018;**100-B**(5):667–74. [PubMed ID: 29701102]. https://doi.org/10.1302/0301-620X.100B5.BJJ-2017-0577.R2.
6. Mauffrey C, Barlow BT, Smith W. Management of segmental bone defects. *J Am Acad Orthop Surg*. 2015;**23**(3):143–53. [PubMed ID: 25716002]. https://doi.org/10.5435/JAAOS-D-14-00018.
7. Brydone AS, Meek D, Maclaine S. Bone grafting, orthopaedic biomaterials, and the clinical need for bone engineering. *Proc Inst Mech Eng H*. 2010;**224**(12):1329–43. [PubMed ID: 21287823]. https://doi.org/10.1243/09544119JEIM770.
8. Pruss A, Seibold M, Benedix F, Frommelt L, von Garrel T, Gurtler L, et al. Validation of the 'Marburg bone bank system' for thermodisinfection of allogenic femoral head transplants using selected bacteria, fungi, and spores. *Biologicals*. 2003;**31**(4):287–94. [PubMed ID: 14624799]. https://doi.org/10.1016/j.biologicals.2003.08.002.
9. Katthagen BD, Prub A. [Bone allografting]. *Orthopade*. 2008;**37**(8):764–71. German. [PubMed ID: 18584151]. https://doi.org/10.1007/s00132-008-1272-y.
10. Siemssen N, Friesecke C, Wolff C, Beller G, Wassilew K, Neuner B, et al. [A clinical radiological score for femoral head grafts : Establishment of the Tabea FK score to ensure the quality of human femoral head grafts]. *Orthopade*. 2021;**50**(6):471–80. German. [PubMed ID: 32642941]. [PubMed Central ID: PMC8589819]. https://doi.org/10.1007/s00132-020-03941-5.
11. Mohr J, Germain M, Winters M, Fraser S, Duong A, Garibaldi A, et al. Disinfection of human musculoskeletal allografts in tissue banking: a systematic review. *Cell Tissue Bank*. 2016;**17**(4):573–84. [PubMed ID: 27665294]. [PubMed Central ID: PMC5116033]. https://doi.org/10.1007/s10561-016-9584-3.
12. Moreno M, Amaral MH, Lobo JM, Silva AC. Scaffolds for Bone Regeneration: State of the Art. *Curr Pharm Des*. 2016;**22**(18):2726–36. [PubMed ID: 26845128]. https://doi.org/10.2174/1381612822666160203114902.
13. Dimitriou R, Tsiridis E, Giannoudis PV. Current concepts of molecular aspects of bone healing. *Injury*. 2005;**36**(12):1392–404. [PubMed ID: 16102764]. https://doi.org/10.1016/j.injury.2005.07.019.
14. Lohmann CH, Andreacchio D, Koster G, Carnes DJ, Cochran DL, Dean DD, et al. Tissue response and osteoinduction of human bone grafts in vivo. *Arch Orthop Trauma Surg*. 2001;**121**(10):583–90. [PubMed ID: 11768641]. https://doi.org/10.1007/s004020100291.
15. Foster TE, Puskas BL, Mandelbaum BR, Gerhardt MB, Rodeo SA. Platelet-rich plasma: from basic science to clinical applications. *Am J Sports Med*. 2009;**37**(11):2259–72. [PubMed ID: 19875361]. https://doi.org/10.1177/0363546509349921.
16. Jurk K, Kehrel BE. Platelets: physiology and biochemistry. *Semin Thromb Hemost*. 2005;**31**(4):381–92. [PubMed ID: 16149014]. https://doi.org/10.1055/s-2005-916671.
17. Galasso O, Mariconda M, Romano G, Capuano N, Romano L, Ianno B, et al. Expandable intramedullary nailing and platelet rich plasma to treat long bone non-unions. *J Orthop Traumatol*. 2008;**9**(3):129–34. [PubMed ID: 19384608]. [PubMed Central ID: PMC2656988]. https://doi.org/10.1007/s10195-008-0021-7.
18. Basdelioglu K, Meric G, Sargin S, Atik A, Ulusal AE, Akseki D. The effect of platelet-rich plasma on fracture healing in long-bone pseudoarthrosis. *Eur J Orthop Surg Traumatol*. 2020;**30**(8):1481–6. [PubMed ID: 32617687]. https://doi.org/10.1007/s00590-020-02730-2.
19. Abdullah WA. Evaluation of bone regenerative capacity in rats claverial bone defect using platelet rich fibrin with and without beta tri calcium phosphate bone graft material. *Saudi Dent J*. 2016;**28**(3):109–17. [PubMed ID: 27656077]. [PubMed Central ID: PMC5021816]. https://doi.org/10.1016/j.sdentj.2015.09.003.
20. *Donation and Transplantation: The Code of the Republic of Kazakhstan on the Health of the People and the Healthcare System of July 7, 2020 No. 360. Chapter 24: Donation and Transplantation*. Adilet; 2020. Available from: https://adilet.zan.kz/rus/docs/K2000000360.
21. *Order of the Minister of Health and Social Development of the Republic of Kazakhstan dated 04.05. 2019 on the Approval of the Rules for the Formation and Maintenance of Registers of Tissue Recipients (part of the tissue) and (or) Organs (part of the organs), as well as Tissue Donors (part of the tissue) and (or) Organs (part of organs), Hematopoietic Stem Cells*. Adilet; 2020. Available from: https://adilet.zan.kz/rus/docs/V1500011477.
22. Tuleubaev B, Saginova D, Saginov A, Tashmetov E, Koshanova A. Heat Treated Bone Allograft as an Antibiotic Carrier for Local Application. *Georgian Med News*. 2020;(306):142–6. [PubMed ID: 33130662].
23. Parasuraman S, Raveendran R, Kesavan R. Blood sample collection in small laboratory animals. *J Pharmacol Pharmacother*. 2010;**1**(2):87–93. [PubMed ID: 21350616]. [PubMed Central ID: PMC3043327]. https://doi.org/10.4103/0976-500X.72350.
24. Dohan Ehrenfest DM, Rasmusson L, Albrektsson T. Classification of platelet concentrates: from pure platelet-rich plasma (P-PRP) to leucocyte- and platelet-rich fibrin (L-PRF). *Trends Biotechnol*. 2009;**27**(3):158–67. [PubMed ID: 19187989]. https://doi.org/10.1016/j.tibtech.2008.11.009.
25. National Research Council. *Guide for the care and use of laboratory animals*. 8th ed. Washington, D.C, USA: National Academies Press; 2011.
26. Cruz-Orive LM, Weibel ER. Recent stereological methods for cell biology: a brief survey. *Am J Physiol*. 1990;**258**(4 Pt 1):L148–56. [PubMed ID: 2185653]. https://doi.org/10.1152/ajplung.1990.258.4.L148.
27. Chiu YL, Luo YL, Chen YW, Wu CT, Periasamy S, Yen KC, et al. Regenerative Efficacy of Supercritical Carbon Dioxide-Derived Bone Graft Putty in Rabbit Bone Defect Model. *Biomedicines*. 2022;**10**(11). [PubMed ID: 36359322]. [PubMed Central ID: PMC9687147]. https://doi.org/10.3390/biomedicines10112802.
28. Burkitt HG, Young B, Wheater JW. *Wheater's Functional Histology: A Text and Colour Atlas*. 3rd ed. New York, USA: Churchill Livingstone; 2015.
29. Akeda K, An HS, Okuma M, Attawia M, Miyamoto K, Thonar EJ, et al. Platelet-rich plasma stimulates porcine articular chondrocyte proliferation and matrix biosynthesis. *Osteoarthritis Cartilage*. 2006;**14**(12):1272–80. [PubMed ID: 16820306]. https://doi.org/10.1016/j.joca.2006.05.008.
30. Chien CS, Ho HO, Liang YC, Ko PH, Sheu MT, Chen CH. Incorporation of exudates of human platelet-rich fibrin gel in biodegradable fibrin scaffolds for tissue engineering of cartilage. *J Biomed Mater Res B Appl Biomater*. 2012;**100**(4):948–55. [PubMed ID: 22279009]. https://doi.org/10.1002/jbm.b.32657.
31. Kaps C, Loch A, Haisch A, Smolian H, Burmester GR, Haupl T, et al. Human platelet supernatant promotes proliferation but not differentiation of articular chondrocytes. *Med Biol Eng Comput*. 2002;**40**(4):485–90. [PubMed ID: 12227637]. https://doi.org/10.1007/BF02345083.
32. Gaissmaier C, Fritz J, Krackhardt T, Flesch I, Aicher WK, Ashammakhi N. Effect of human platelet supernatant on proliferation and matrix synthesis of human articular chondrocytes in monolayer and three-dimensional alginate cultures. *Biomaterials*. 2005;**26**(14):1953–60. [PubMed ID: 15576169]. https://doi.org/10.1016/j.biomaterials.2004.06.031.
33. Spreafico A, Chellini F, Frediani B, Bernardini G, Niccolini S, Serchi T, et al. Biochemical investigation of the effects of human platelet releasates on human articular chondrocytes. *J Cell Biochem*. 2009;**108**(5):1153–65. [PubMed ID: 19731249]. https://doi.org/10.1002/jcb.22344.
34. Cullinane DM. The role of osteocytes in bone regulation: mineral

homeostasis versus mechanoreception. *J Musculoskelet Neuronal Interact*. 2002;**2**(3):242–4. [PubMed ID: 15758444].
35. Bonewald LF. The amazing osteocyte. *J Bone Miner Res*. 2011;**26**(2):229–38. [PubMed ID: 21254230]. [PubMed Central ID: PMC3179345]. https://doi.org/10.1002/jbmr.320.
36. Neve A, Corrado A, Cantatore FP. Osteocytes: central conductors of bone biology in normal and pathological conditions. *Acta Physiol (Oxf)*. 2012;**204**(3):317–30. [PubMed ID: 22099166]. https://doi.org/10.1111/j.1748-1716.2011.02385.x.
37. Kennedy OD, Herman BC, Laudier DM, Majeska RJ, Sun HB, Schaffler MB. Activation of resorption in fatigue-loaded bone involves both apoptosis and active pro-osteoclastogenic signaling by distinct osteocyte populations. *Bone*. 2012;**50**(5):1115–22. [PubMed ID: 22342796]. [PubMed Central ID: PMC3366436]. https://doi.org/10.1016/j.bone.2012.01.025.
38. Qiu S, Rao DS, Fyhrie DP, Palnitkar S, Parfitt AM. The morphological association between microcracks and osteocyte lacunae in human cortical bone. *Bone*. 2005;**37**(1):10–5. [PubMed ID: 15878702]. https://doi.org/10.1016/j.bone.2005.01.023.
39. Pajevic PD, Spatz JM, Garr J, Adamson C, Misener L. Osteocyte biology and space flight. *Curr Biotechnol*. 2013;**2**(3):179–83. [PubMed ID: 25346885]. [PubMed Central ID: PMC4205970]. https://doi.org/10.2174/22115501113029990017.
40. Martin RB. Toward a unifying theory of bone remodeling. *Bone*. 2000;**26**(1):1–6. [PubMed ID: 10617150]. https://doi.org/10.1016/s8756-3282(99)00241-0.
41. Gu G, Mulari M, Peng Z, Hentunen TA, Vaananen HK. Death of osteocytes turns off the inhibition of osteoclasts and triggers local bone resorption. *Biochem Biophys Res Commun*. 2005;**335**(4):1095–101. [PubMed ID: 16111656]. https://doi.org/10.1016/j.bbrc.2005.06.211.
42. Dickson K, Katzman S, Delgado E, Contreras D. Delayed unions and nonunions of open tibial fractures. Correlation with arteriography results. *Clin Orthop Relat Res*. 1994;(302):189–93. [PubMed ID: 8168299].
43. Brownlow HC, Reed A, Simpson AH. The vascularity of atrophic non-unions. *Injury*. 2002;**33**(2):145–50. [PubMed ID: 11890916]. https://doi.org/10.1016/s0020-1383(01)00153-x.
44. Trueta J. The Role of the Vessels in Osteogenesis. *J Bone Joint Surg*. 1963;**45-B**(2):402–18. https://doi.org/10.1302/0301-620x.45b2.402.